

Climate warming and cooling feedbacks from boreal forest fires

Max J. van Gerrevink¹, Sander Veraverbeke^{1,2}, Sol Cooperdock³, Stefano Potter³, Qirui Zhong¹, Michael Moubarak⁴, Scott J. Goetz⁵, Michele C. Mack⁶, James T. Randerson⁷, Nick Schutgens¹, Merritt R. Turetsky⁸, and Brendan M. Rogers³

¹Faculty of Science, Vrije Universiteit Amsterdam, Amsterdam, the Netherlands, ²School of Environmental Sciences, University of East Anglia, Norwich, United Kingdom, ³Woodwell Climate Research Center, Falmouth, MA, USA, ⁴Hamilton College, Hamilton, NY, USA, ⁵School of Informatics, Computing, and Cyber Systems, Northern Arizona University, Flagstaff, AZ, USA, ⁶Center for Ecosystem Science and Society, Northern Arizona University, Flagstaff, AZ, USA, ⁷Department of Earth System Science, University of California, Irvine, CA, USA, ⁸University of Colorado Boulder, Boulder, CO, USA

Climate feedbacks from boreal fires

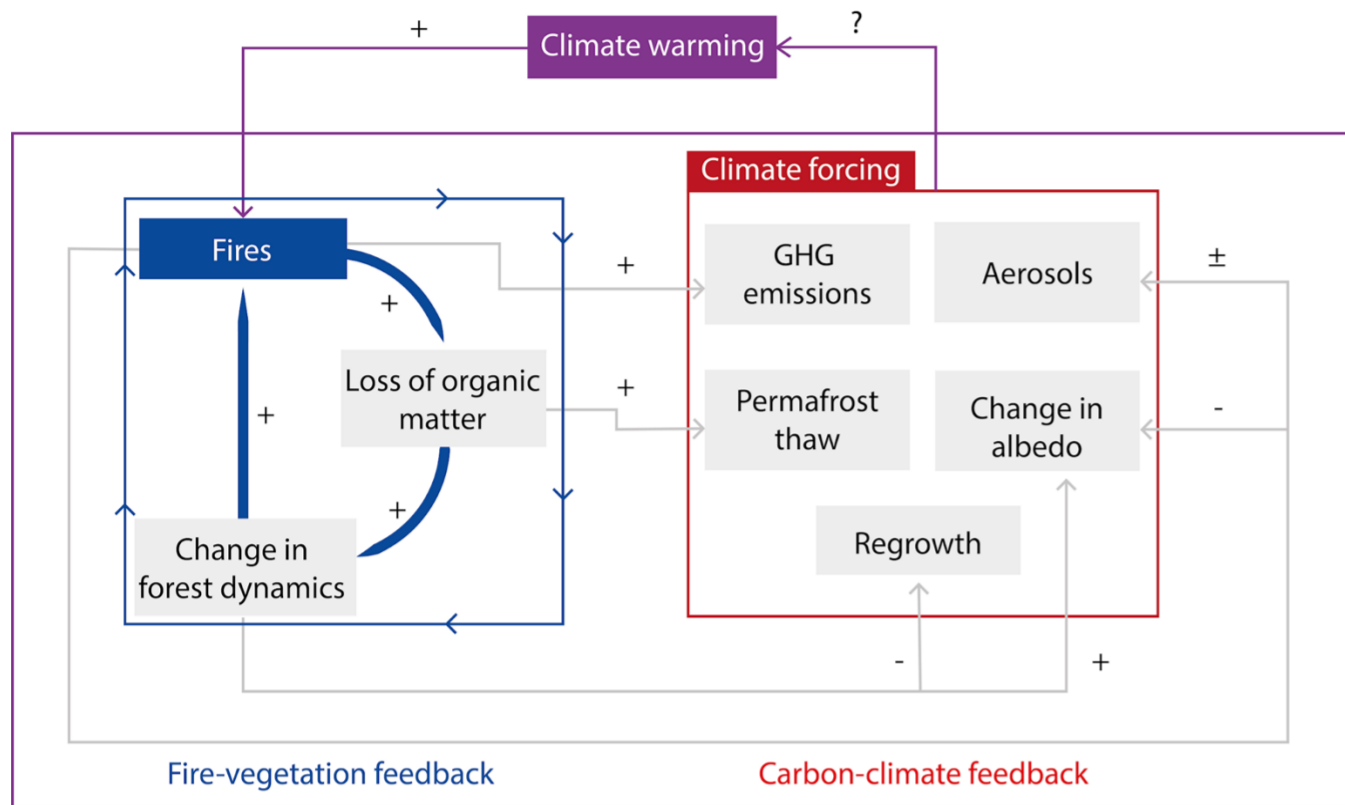


Fig.1 Schematic illustration of climate feedback mechanisms from boreal fires.

Methods

Our radiative forcing estimates – in units of W/m^2 of burned area – capture climate feedbacks up to a 70-years post-fire environment in at 500m high-resolution using shared socioeconomic pathway SSP2-4.5.

- *Greenhouse gases and Precursors*: temporal-explicit equation and interpolation between greenhouse warming potentials
- *Aerosols*: output derived from atmospheric chemistry models
- *Permafrost emissions*: first-order estimates based on carbon release curves upon thaw with soil organic carbon profiles, permafrost probability, and changes in active layer thickness.
- *Changes in Albedo*: modelled post-fire albedo trajectories based on random forest models. Results were translated in radiative forcing using spatial explicit albedo kernels.
- *Vegetation recovery*: modelled net ecosystem exchange with random forest models.

Spatiotemporally explicit radiative forcing estimates

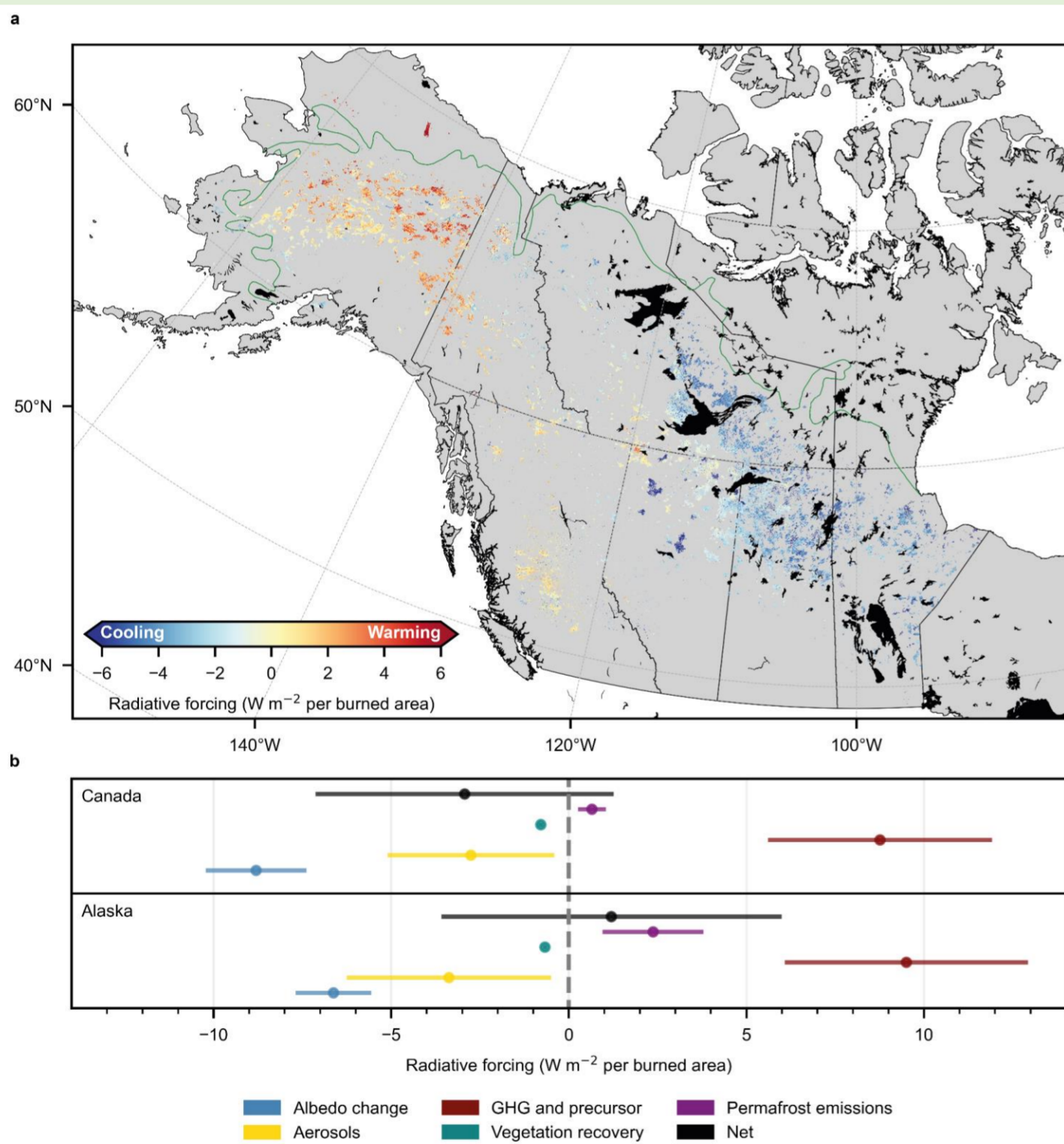


Fig. 2 Climate Radiative forcing from across Alaska and western Canada. Pixel-based radiative forcing estimates for high-latitude fires in the ABoVE domain between 2001 and 2019. a, Net radiative forcing map for the 70-year post-fire environment, positive values (warming feedback) are displayed in red, negative values (cooling feedback) are displayed in blue. b, Contribution plot of direct emissions through greenhouse gas and precursors (maroon) and aerosols (gold), secondary emissions related to permafrost emissions (purple), post-fire changes in surface albedo (blue), and post-fire carbon accumulation during the successional phase for Alaskan and Canadian fires. Gray bars indicate the spatial variability of each feedback mechanism.

Conclusions

- Averaged over 70-years, net radiative forcing across Alaskan fires shows climate **warming** ($1.20 \pm 4.79 W/m^2$), while Canadian fires show on average a climate **cooling** ($-2.94 \pm 4.20 W/m^2$) effect.
- We demonstrate the significant role the permafrost-carbon feedback has in the net climate warming effects of fires and is crucial in the warming from Alaskan fires.
- Net radiative forcing trends are dominated by cooling effect from prolonged spring snow cover.
- High fuel consumption and permafrost thaw leads to climate warming fires.

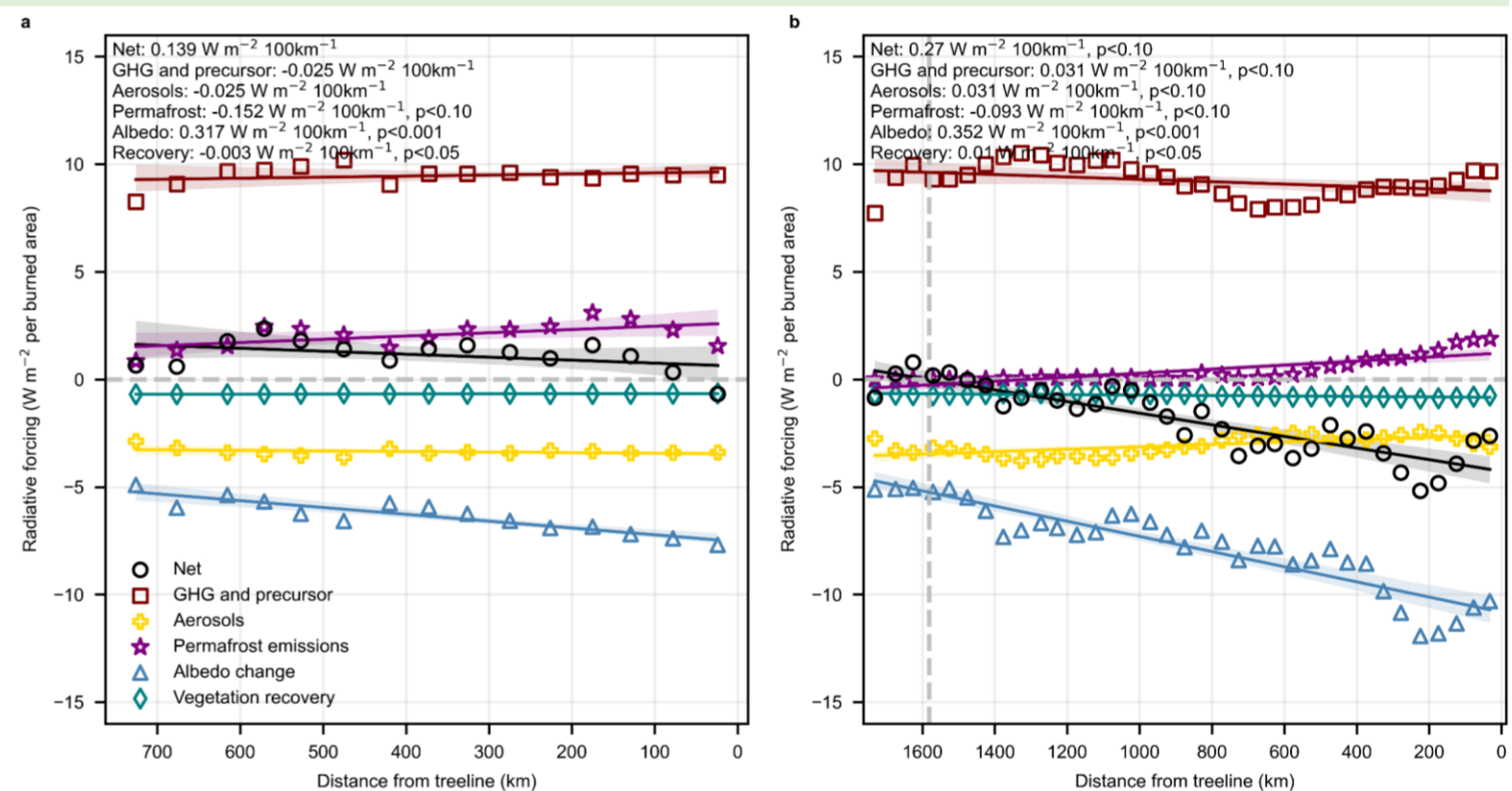


Fig. 3 Trends in radiative forcing in relation to distance from treeline and month of ignition. a, Distance from treeline plot (binned to 50 km) for Alaska and b, for Canada. c, mean warming and cooling feedbacks across the fire season for Alaska and d, for Canada. Net (black circles), Greenhouse gases and precursors (maroon squares), aerosols (gold pluses), permafrost (purple stars), albedo (light blue triangles), and vegetation recovery (teal diamonds). All individual trends with slope (in $W m^{-2} 100km^{-1}$ and $W m^{-2} month^{-1}$) are provided, and p represent significant correlations.

Drivers of warming fires

Fig. 4 Burn depth and total carbon losses. a, Burned area of on average climate warming fires (red; $n = 233$) has burned deeper into the soil organic layer than on average climate cooling fires (blue; $n = 437$) ($p < 0.001$). b, Average ecosystem carbon pool losses after fire across climate warming (red; $n = 96$) and climate cooling fires (blue; $n = 380$). Darker colors represent the belowground carbon pools, lighter represent the aboveground carbon pools. The errors bars represent the standard deviation of carbon pool losses (grey; belowground, and silver; aboveground). Letters represent significant differences ($p < 0.001$) between the two groups within the above- and belowground pools.

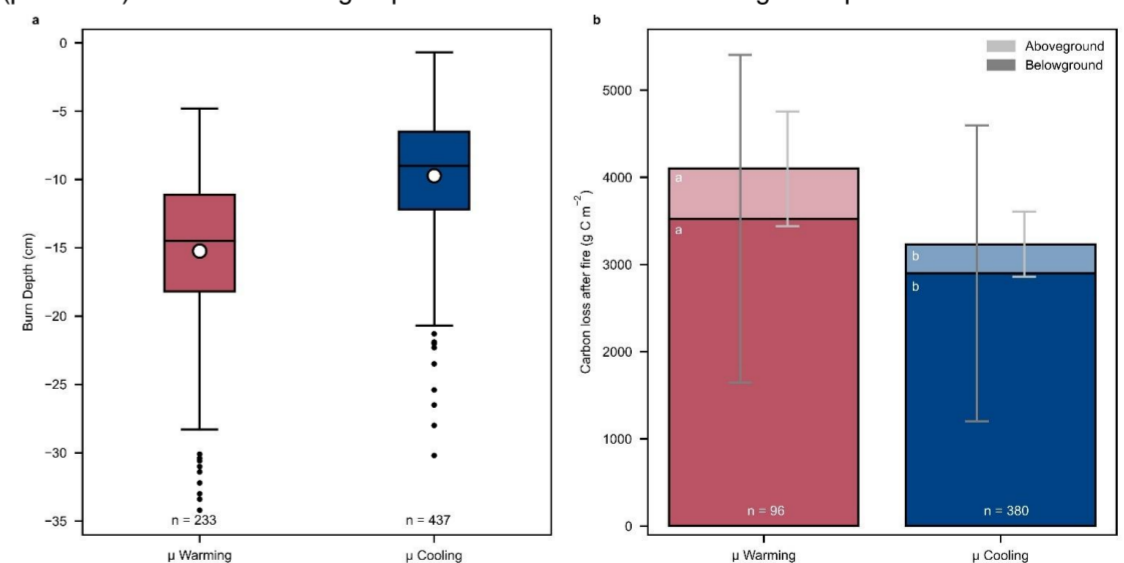


Table. 1 Influence of landscape characteristics on climate warming and cooling fires.

Variable	$\mu_{warming\ fires} (\pm s.d.)$	$\mu_{cooling\ fires} (\pm s.d.)$	P-value
Net radiative forcing	2.40 (± 2.04) W/m^2	-3.14 (± 4.14) W/m^2	<0.001
Moisture class	Subxeric to mesic	Mesic	0.032
Slope	5.92 (± 6.79) $^\circ$	2.09 (± 4.99) $^\circ$	<0.001
Elevation	537.47 (± 230.99) m	309.57 (± 109.44) m	<0.001
Stand density	0.71 (± 0.61) stems/ m^2	0.68 (± 0.72) stems/ m^2	0.77
Stand age	98 (± 51) years	96 (± 48) years	0.696
Fraction black spruce	0.86 (± 0.27)	0.72 (± 0.36)	<0.001
Day of burning	193 (± 23) day of year	195 (± 21) day of year	0.111
Burn depth	15.24 (± 6.03) cm	9.63 (± 4.44) cm	<0.001
Total C combustion	4.099 ± 2.144 g C/ m^2	3.232 ± 1.743 g C/ m^2	<0.001